Journal of Applied Polymer Science

Improved specific thermomechanical properties of polyurethane nanocomposite foams based on castor oil and bacterial nanocellulose

Rocío Belén Gimenez,[1] Luciano Leonardi,[1] Patricia Cerrutti,[1,2] Javier Amalvy,[3] Leonel Matías Chiacchiarelli[1]

[1]Instituto de Tecnología de Polímeros y Nanotecnología (ITPN), CONICET-UBA, Buenos Aires, Argentina
[2]Departamento de Ingeniería Química, Facultad de Ingeniería, UBA, Buenos Aires, Argentina
[3]Instituto de Investigaciones Fisicoquímicas Teóricas y Aplicadas (INIFTA), CCT CONICET La Plata—UNLP, La Plata, Buenos Aires, Argentina
Correspondence to: L. M. Chiacchiarelli (E-mail: lmchiacchiarelli@yahoo.com.ar)

ABSTRACT: Bacterial nanocellulose (BNC) was used to synthesize polyurethane foams (PUFs) prepared from castor oil polyol and MDI diisocyanate using water as the blowing agent. The BNC reacted with the isocyanate, increasing the weight content of urethane hard segments (HS). It did not behave as a nucleation agent, forming a nanometric distribution of cells within the struts followed by a reduction of the apparent density (−7.6%) and a relevant increase of cell size in the growth direction (+37.9%). An alignment of the BNC parallel to the cell walls was observed, producing a nanocomposite with a higher reinforcement weight fraction in that area. At only 0.2 wt %, the BNC behaved as a nanostructured reinforcement, improving the specific compression modulus and strength by +4.67% and +23.6%, respectively, as well as the thermomechanical properties, with an improvement of the specific E' at 30 °C of +52.4%. © 2017 Wiley Periodicals, Inc. J. Appl. Polym. Sci. **2017**, *134*, 44982.

KEYWORDS: bacterial nanocellulose; foams; polyurethane; thermomechanical properties

Received 7 December 2016; accepted 6 February 2017
DOI: 10.1002/app.44982

INTRODUCTION

Polyurethane foams (PUFs) represent a class of materials which have a fundamental role in the modern society.[1] In the majority of applications, both precursors are obtained from nonrenewable resources, such as ethylene gas. Substantial research has been focus on the development of precursors obtained from renewable resources, such as polyols from triglycerides (natural oils).[2–6] Of all the types of natural oils used, castor oil has been the one which has been mostly studied. On the other hand, research associated to bio-based alternatives of the isocyanate precursor had not led to industrially viable applications.[6–10] Still today, most commercial isocyanates are synthesized from benzene.

Soft, semi-rigid, and rigid PUFs are obtained after using precursors with different molecular weights, functionality, and chemical nature. For the case of a rigid PUF, which is the main focus of this work, the HS has a fundamental role because the mechanical properties of the PUF are mainly ascribed to its chemical and physical nature. To formulate a rigid PUF it is desirable to have a microstructure where the properties of the HS are preponderant. To achieve this, polyols with low molecular weights and high functionalities are used. This leads to a very high weight content of the isocyanate precursor because a high isocyanate index is also desirable to homopolymerize the isocyanate precursor or to react all the hydroxyl groups present in highly functional polyols. Then, the renewable content of the PUF is limited because replacing the polyol precursor is not as relevant as to replace the isocyanate precursor. An alternative to solve this relevant issue is to introduce nanoparticles within the microstructure which act as a HS. The advantage of using nanotechnology is that these nanoparticles can be used to manufacture nanocomposites, where a very small fraction of nanoparticles (<1 wt %) are incorporated in the synthesis path so as to obtain a substantial improvement of specific properties. Another advantage is that if the nanoparticles that are used are obtained from renewable resources and behave as HS, the PUF could be reformulated with a lower content of the isocyanate precursor so as to have similar thermomechanical properties. The overall effect is to have a rigid PUF with a lower content of isocyanate precursor and to increase significantly the renewable content of the PUF.

Several nanoparticles can be used to obtain polyurethane nanocomposites.[11–24] One of the most relevant nanoparticles

obtained from renewable resources is nanocellulose. Its precursor, cellulose, is one of the most abundant renewable resources on earth and extensive research in the last decade has lead to several industrial applications.[25–39] To obtain nanocellulose, several processing paths have arisen. The most relevant ones are associated to the acid-hydrolysis or the bacterial production from renewable carbon sources. The first one is denominated as nanocrystalline cellulose (CNC) while the second one is termed bacterial nanocellulose (BNC). Further details of these paths can be consulted elsewhere.[25–34,40,41] Our research group has already published several articles regarding the synthesis and functionalization of BNC nanoparticles.[34,42–45] As noticed by a recent review,[46] the formulation of PUFs reinforced with CNC[47–57] has been previously studied. On the other hand, so far, no publication has dealt with the incorporation of BNC in a PUF formulation. Articles regarding the formulation of solid PU reinforced mostly CNC and a few with BNC are available in literature.[5,58–60] A comprehensive analysis comparing the effect of different nanoparticles on the mechanical properties of PUF has been recently published by Lobos and Velankar.[50]

In this work, water blown PUFs synthesized from MDI isocyanate and a bio-based castor oil polyol were formulated with BNC using the "Polmix"[61] route at a fixed concentration of 0.2 wt %. Characterization of the PUFs compromised cell size dimensions, anisotropy factor, fracture surface analysis, BNC orientation using scanning electron microscopy (SEM); apparent density, compressive mechanical properties, storage, and damping factor as a function of temperature using dynamical mechanical analysis (DMA); thermal transitions using differential scanning calorimetry (DSC), chemical structure by means of Fourier transform infrared spectroscopy (FTIR) and thermal stability using thermogravimetric weight loss analysis (TGA).

EXPERIMENTAL

Materials

Methylene diphenyl diisocyanate (MDI, Suprasec 9561) were used as received. It had a functionality of 2.70 and a NCO number of 21.0. This last value was determined using the procedure of the ASTM D2572 standard. Before each experiment, the isocyanate number (NCO number) of the isocyanate batch was measured so as to corroborate that relevant changes on the NCO number did not occur. Castor oil (CO), obtained from Parafarm (99.9%), was used as the polyol (CO), with an hydroxyl value (#OH) of 157 mg KOH mg^{-1} determined by acetylation with acetic anhydride in pyridine solution, according to the ASTM D4274–99 (Test Method A). To obtain a polyol with a higher #OH (CO_{450}), the procedure reported by Cordero *et al.*[58] was implemented. In short, the CO, dry triethanolamine and lithium hydroxide were added in a reactor and mixed at room temperature using a mechanical stirrer. The temperature was raised to 150 °C in 0.5 h and it was maintained at this value for 2.5 h. The castor oil:triethanolamine molar ratio was 1:1 and the catalyst was used in a 0.2 wt % based on the total reactants. The measured #OH of the synthesized CO_{450} was 452.15 mg KOH mg^{-1}. A silicone surfactant, commercially known as Niax L-585, was obtained from Resikem. Dibutyltin dilaurate (DBTDL, 95%) was kindly supplied by Mentvil Argentina. Distilled water (18.2 MΩ) was used as the blowing agent.

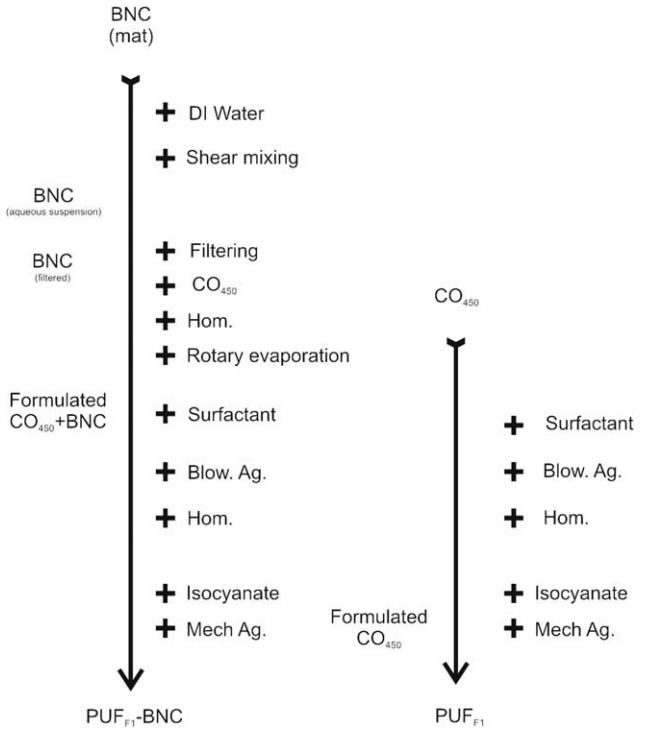

Figure 1. Scheme of the experimental procedure used for the preparation of PUF_{F1} (right) and PUF_{F1}-BNC (left).

BNC was produced by a strain of *Gluconacetobacter xylinus* gently provided by Dr. Luis Lelpi (Fundación Instituto Leloir, Buenos Aires, Argentina). Static fermentations were carried on for 14 days in Hestrin and Schramm medium[62] modified by replacing D-glucose by the same concentration of glycerol (Biopack) at 28 ± 1 °C, maintaining a ratio "volume flask: volume medium" of 5:1. The pellicles of BNC, from now on denominated BNC mat, were rinsed with water to remove the culture medium and then boiled in 2% w/v sodium hydroxide (NaOH) solution for 1 h in order to eliminate the bacterial cells from the cellulose matrix. Finally, the BNC mat was washed with distilled water till neutralization.

Sample Preparation Procedures

A scheme of the preparation procedures of the PUFs prepared in this work is depicted in Figure 1. PUFs were prepared with the formulation PUF_{F1} using isocyanate at 192 parts by weight (pbw), CO_{450} at 100 pbw, blowing agent at 1 pbw, surfactant at 1 pbw, and a fixed isocyanate index of 105. For the case of the PUF_{F1}-BNC 0.2 wt % and PUF_{F1}-BNC 0.5 wt % the BNC nanoparticle was added at 0.6 and 1.5 pbw, respectively. This represented a typical formulation of a rigid PUF, where the highly reactivity of the CO_{450} deemed unnecessary the use of additional catalysts. For both formulations, an isocyanate index of 105 was implemented. The experimental procedure consisted on the 'one shot' method whereas the formulated polyol is mixed intensively with the isocyanate. To obtain a homogeneous mixture of the formulated polyol, a homogenizer (Proscientific) was utilized for 1 min at 15,000 rpm after all the components

were introduced in the beaker. Then, the formulated polyol and the isocyanate precursors were poured in a HDPE cylindrical mould with an internal diameter of 70 mm and dispersed with a Cowles stirrer rotating at 2000 rpm for 30 s. To measure the temperature evolution of the foaming process, a K type thermocouple with a data logger (TES 1307) was inserted in the internal perimeter of the mold. To corroborate the reproducibility of the results, three samples were done for each formulation.

The experimental procedure for the preparation of the PUF_{F1}-BNC started with the BNC mat (Figure 1). According to thermal studies and weight loss measurements, the actual BNC content within the mat was approximately 2.24 wt %. Due to the continuous nature of the mat, it was necessary to break down this initial morphology by the application of a shear force under a diluted aqueous solution. Hence, the required amount of mat (19.46 g) was introduced in a DI water beaker at 15 wt % (127 g H_2O). Subsequently, a shear mixer device (Sparmix) was used for 10 min. After this processing step, the continuous nature of the mat was broken and the BNC formed a colloidal suspension in DI water with a concentration of 0.34 wt %. Subsequently, the aqueous dispersion was vacuum filtered so as to reduce significantly the BNC dilution. To corroborate that the filtering process did not removed BNC from the solution, an aliquot of the DI water after filtering was taken and dried in an oven. Weight measurements indicated that no significant amounts of BNC were removed from the solution. After this stage, the required amount of polyol was added (40 g. of CO_{450}) following a homogenization procedure with a ProScientific device at 15,000 rpm for 10 min, separated in intervals of 5 min to avoid a substantial temperature increase. Finally, a rotary evaporator (Senco R206) was used so as to completely remove the water content of the dispersion. After this procedure, a polyol formulated with BNC was obtained. Finally, an identical experimental procedure was applied so as to obtain the PUF_{F1}-BNC.

Sample Characterization Techniques

Apparent density was measured by cutting squares of 1 cm sides and by measuring its weight. Twenty-five samples of each formulation were used to elaborate the statistics. The fracture surface of the PUFs, obtained by cryogenic fracture, was analyzed with SEM (Supra Zeiss 25). Before the analysis, the samples were gold sputtered. Compressive mechanical analysis was performed with an Instron 5985 universal testing machine, following the guidelines of the standard ASTM D1621. Twenty-five samples were tested for each formulation. FTIR absorption spectra were obtained with a Shimadzu IRAffinity using the Attenuated Total Reflection (ATR) methodology (ZnSe prism with and incidence angle of 45° and 10 reflections). It is important to notice that the dimensions of the prism were approximately 10 mm by 100 mm, hence, for each measurement, a wide sample area was covered. Each spectrum was obtained from 60 scans at a resolution of 4.0 cm^{-1} and corrected for ATR. The absorption spectra were normalized using the band of the phenyl group, centered at approximately 1595 cm^{-1}. TGA analysis was performed using Shimadzu TGA 50 under a nitrogen atmosphere. The thermal experiment started at room temperature and went up to 800 °C at a constant rate of 10 °C min^{-1} with three samples tested for each formulation. DSC was performed with a Shimadzu DSC-60. To obtain the thermal transitions of the formulations, a full thermal cycle was implemented which consisted of three thermal cycles. The first one started at −60 °C and went up to 200 °C at a scan rate of 10 °C min^{-1}. The second one started at 200 °C and went down to −60 °C at 15 °C min^{-1} and, finally, the third one was identical to the first cycle. DMA was carried out with a Perkin & Elmer DMA 8000. The compression mode was used, fixing the oscillation frequency to 1.0 Hz and the amplitude to 0.001 mm. The thermal scan started at 20 °C and went up to 180 °C at a scan rate of 2 °C min^{-1}. It was corroborated that the experiments fell into the linear viscoelastic region of the material. At least three samples were tested for each formulation. To further corroborate the results, additional DMA analyses were performed under flexural conditions, fixing the oscillation frequency to 1.0 Hz, the amplitude to 0.001 mm and with a thermal scan starting at 0 °C and going up to 180 °C at a scan rate of 2 °C min^{-1}.

RESULTS AND DISCUSSION

It is important to highlight that specific hypothesis obtained from each experimental technique will be correlated and tested taking into account the results of other experimental methods. The reader is prompted to read the entire section so as to understand which are the most substantiated hypothesis of this scientific work.

A crucial aspect of formulating a PUF with BNC is to select a specific processing route. As already noticed by Kenny *et al.*,[61] the processing route (which is not the processing method) has a profound effect on the final properties of the PU. In this work, the authors have decided to use the "Polmix"[61] route, in which the BNC is formulated within the polyol precursor. To obtain a polyol formulated with BNC using that route, the chemical and physical nature of the BNC and the polyol have to be taken into account. The objective is to obtain a stable colloidal dispersion of the BNC in the polyol. To achieve this, one critical factor is to match the hydrophobic or hydrophilic character of both the polyol and the BNC.[63] As far as the BNC is concerned, it is known that nonfunctionalized BNC has a strong hydrophilic character.[34] This property is mainly caused by hydrogen type interactions associated to its hydroxyl functionality. From a theoretical point of view, it is possible to calculate the #OH of BNC considering the molecular structure of the anhydroglucose unit (AGU). Assuming that the AGU has 3 moles of hydroxyl groups, it can be deduced that the BNC would have a #OH of 887.7 mg KOH mg^{-1}. Taking into account this value and considering the hydrophilic nature of polyols, it can be inferred that the native BNC is more suitable to formulate semi-rigid or rigid PUF. In these formulations, polyols with a high #OH value are frequently employed. Hence, a better match between the hydrophilic nature of the BNC and the polyol is obtained. This can be translated in a stable colloidal dispersion of the BNC in the polyol. The polyol used in this work was a bio-based polyol, obtained from CO, which had and #OH equal to 157 mg KOH mg^{-1}. However, for rigid and semi-rigid PUF, it is imperative to use polyols with a higher #OH. For this reason, the CO was

Table I. Geometrical and Mechanical Properties of the PUF Samples

PUF type	Cream time (s)	T_{peak} (°C)	Final height (cm)	ρ_{AVG} (kg m^{-3})	Cell size (μm)	A.F.	E_c. ρ_{AVG}^{-1} (J g^{-1})	σ_c. ρ_{AVG}^{-1} (J g^{-1})
PUF_{F1}	122 ± 15	77.7	119 ± 1.0	$9.76.10^1 \pm 8.00$	L: $3.83.10^2 \pm 90.6$. T: $2.61.10^2 \pm 60.2$	1.47	$1.07.10^1 \pm 2.2.10^{-4}$	$4.75 \pm 8.6.10^{-2}$
PUF_{F1}-BNC 0.2 wt %	50 ± 12	65.0	117 ± 1.5	$9.02.10^1 \pm 5.1$	L: $5.28.10^2 \pm 162$. T: $2.44.10^2 \pm 77.7$	2.16	$1.12.10^1 \pm 3.1.10^{-4}$	$5.87 \pm 2.2\text{-}10^{-2}$
PUF_{F1}-BNC 0.5 wt %	10 ± 5	45.0	N.M.	N.M.	N.M.	N.M.	N.M.	N.M.

functionalized so as to obtain a CO with an #OH of 452.15 mg KOH mg^{-1} (CO_{450}).

Previous research has dealt with the effect of different nanoparticles on the thermomechanical properties of PUFs.[32,47,48,55] However, most of it did not consider that the nanoparticles might change the isocyanate index (or NCO index) of the PUF due to the presence of additional reactive groups that compete to react with the isocyanate when added into the formulation. This is a relevant aspect because if the nanoparticles alter the NCO index of the formulation, then, it has to be considered that the resulting thermomechanical properties will be affected not only by the introduction of nanoparticles in the formulation, but also for a change of the NCO index. Following this argument, to properly evaluate the thermomechanical properties of the PUFs, it is necessary to analyze if the hydroxide groups added in the formulation by the BNC would change the NCO index of the formulation. This analysis can be performed using the theoretical #OH value obtained as indicated above and the following equation:

$$w_{iso} = NCO_{index} \frac{4200}{NCO_{number}} \left[\frac{OH_1}{eqw_{OH_1}} + \ldots + \frac{OH_i}{eqw_{OHi}} \right] \quad (1)$$

where w_{iso} represents the amount of isocyanate (g) needed to obtain a PUF with a specific NCO_{index}, NCO number and with i components which contribute hydroxide groups in the formulation. Taking into account that in this work the BNC concentration is in the order of 1 wt % of the total formulation mass, it can be calculated that the fraction $OH_{(BNC)}/eqw_{(BNC)}$ was 0.016. Taking into account that the added contribution of the other components is 0.91, it can be deduced that the contribution of OH groups by the BNC would change at most the NCO_{index} by 1.75%. Since this variation is not significant, it can be deduced that the BNC did not have a relevant effect on the NCO_{index} of the PUF formulation.

Foaming Behavior and Apparent Density

Controlling the chemical and physical phenomena taking place during the formation of a PUF is crucial to obtain a semi-rigid PUF.[1] Any change in the formulation might alter the relative kinetics of the blowing or gelling reactions to such an extent that the stages of cell formation and stabilization could be altered significantly. For example, if any change in formulation might induce a significant decrease of the gelling kinetics, the expanding foam will not develop a self-supporting capability. For the case of a rigid PUF, if the final conversion degree is not high enough, the PUF would not acquire sufficient strength to withstand the pressure difference generated during foaming. In this work, to evaluate the foaming behavior, an *in situ* thermocouple was used to obtain estimates of the cream time and peak temperature during rise. The results are reported in Table I and the temperature evolution is depicted in Figure 2 (for clarity issues only one experiment of each formulation is depicted). The temperature evolution of the PUF_{F1} and the one formulated with 0.2 and 0.5 wt % of BNC are depicted. In this figure, time zero represented the addition of the formulated polyol in the mould (arrow denoted as "a" in Figure 2). The addition of the isocyanate in the mould with the simultaneous initialization of the dispersion procedure was denoted with a "b" arrow.

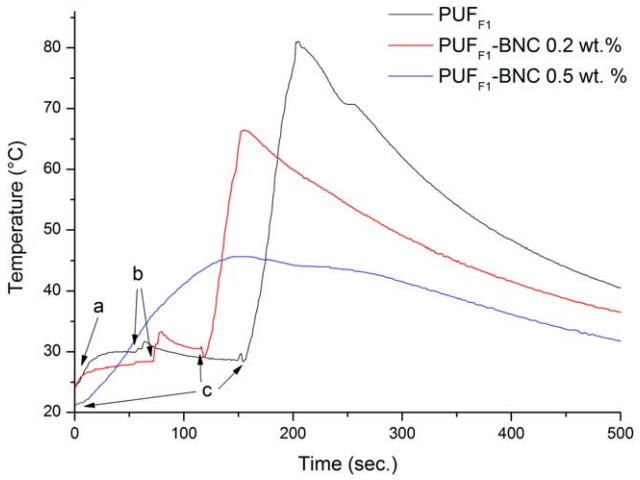

Figure 2. *In situ* temperature-time evolution of the foaming process as a function of BNC weight content (PUF_{F1}, PUF_{F1}-BNC 0.2 wt % and PUF_{F1}-BNC 0.5 wt %). The phenomena indicated by the arrows a, b, and c are explained in the main text. [Color figure can be viewed at wileyonlinelibrary.com]

The chemical and physical phenomena took place after the time denoted by this arrow. Finally, the arrow denominated as "c" denoted the cream time of each experiment. The temperature evolution of the PUFs in this work followed what is typically encountered in literature. The initial steep rise in temperature was ascribed to the cream time of each PUF. It is variation as a function of increasing BNC content in the formulation can also be deduced from Figure 2, where the three different experiments represented the *in situ* temperature profile of the PUF_{F1}, PUF_{F1}-BNC 0.2 wt % and the PUF_{F1}-BNC 0.5 wt %, respectively. Comparing the values of Table I and what it is visualized from Figure 2, it can be deduced that an increase of BNC content in the formulation caused a monotonous decrease of the cream time. Another relevant aspect to notice is that the peak temperature rise (T_{peak}) followed also a monotonous decrease as a function of increasing BNC content. These results highlight that the BNC did not behave solely as inert filler but, to the contrary, as a catalyst. More specifically, the kinetics of the reaction of the hydroxyl groups present in the BNC were probably faster than the hydroxyl groups present in the CO_{450}. The foaming process of the PUFs can be summarized by two main reactions taking place, a gelling reaction and a blowing reaction. In this specific formulation, the gelling reaction is also composed by the formation of an interpenetrated network (IPN) of urethane, urea, and isocyanurate molecules. On the other hand, the blowing reaction was only associated to the reaction of isocyanate with water, forming carbon dioxide and amines (no physical blowing agent was added in the formulation). Going back to the gelling reaction, it is known that if the IPN has a higher relative weight of urea groups, then, a higher exothermic polymerization process will certainly take place.[1] Following this argument, a hypothesis can be established to explain the effect of the addition of BNC in the formulation. Specifically, it can be hypothesized that the addition of BNC caused a substantial decrease of the rate of formation of the urea network in expense of the formation of a urethane network. This hypothesis is also supported by the fact that BNC has a high #OH and a high surface area, indicating that the isocyanate has a strong tendency to react with the hydroxyl groups of the BNC instead of the ones of the castor oil polyol. Another aspect which supports this hypothesis is the fact that the cream time decreased as a function of increasing BNC content. Inert fillers have the tendency to decrease the exothermic peak temperature during foaming but also increase the cream time.[64] On the contrary, for the case of the BNC, the cream time decreased as a function of increasing BNC content. Finally, another observation which supported this hypothesis is related to the fact that the PUF_{F1}-BNC 0.5 wt % was extremely brittle (friable). Taking into account that the urea network is the main contributor to the formation of segregated hard segments which contribute to load-bearing properties, the friability can be explained assuming an IPN which had a higher weight fraction of urethane groups instead of urea. The friability of the PUF_{F1}-BNC 0.5 wt % prevented any further characterization of the foam.

The apparent densities of the PUFs prepared in this work are reported in Table I. For the case of the PUF_{F1}, an average density of 97.6 kg m^{-3} was measured, indicating that a semi-rigid PUF was obtained. On the other hand, for the case of the PUF_{F1}-BNC 0.2 wt %, the average density was 90.2 kg m^{-3}. Then, the incorporation of BNC in the formulation caused a decrease of 7.6% of the average density of the PUF. Further discussion about this interesting result can be found within the fracture surface analysis section.

Infrared Absorption Spectra

The absorption spectra of the PUF_{F1} and the $PUF_{F1\text{-}0}$.2 wt % are depicted in Figure 3. Both spectra showed the typical absorption bands of PU-based materials. The band of the phenyl group was centered at 1595 cm^{-1} (it was used to normalize the spectra). At both 1200 cm^{-1} and 1700 cm^{-1} the absorption bands of the urethane groups were found. The isocyanurate band was centered at approximately 1410 cm^{-1} while the urea groups were found at 1510 cm^{-1}. Other absorption bands were

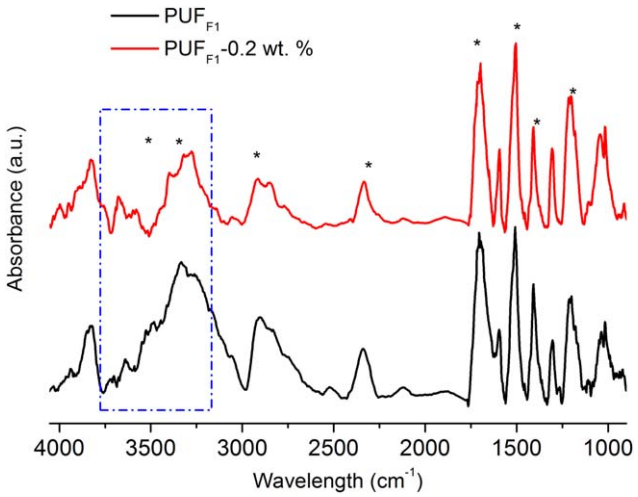

Figure 3. ATR-FTIR absorption spectra of the PUF_{F1} (bottom) and the PUF_{F1}-BNC 0.2 wt % (top). [Color figure can be viewed at wileyonlinelibrary.com]

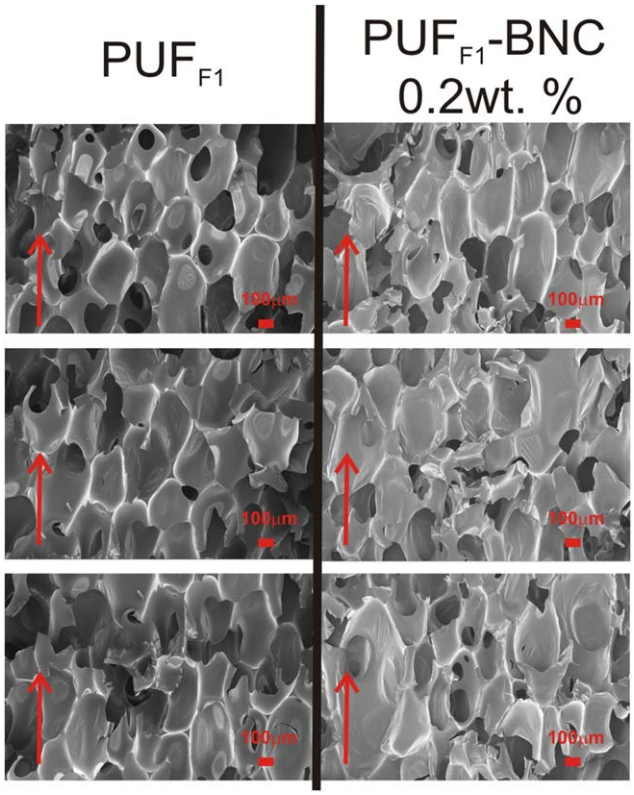

Figure 4. SEM images of the fracture surface at low magnification (150×) of three regions of the PUF_{F1} (left column) and the PUF_{F1}-BNC 0.2 wt % (right column). [Color figure can be viewed at wileyonlinelibrary.com]

found at 2330, 2935, 3480, and 3320 cm^{-1}, which corresponded to CO_2(g) molecules, C—H stretching and the free and H bonded —NH stretching modes, respectively. The samples were measured without milling the foams in a powder form. Hence, it was logical to find the absorption band of CO_2(g). The results emphasize the complex nature of the PUF, composed of numerous chemical groups and not only of a urethane network. Following the analysis of Li *et al.*,[52] for the case of the PUF_{F1}-BNC 0.2 wt %, the absence of an absorption band centered at 3480 cm^{-1} supported the hypothesis that the isocyanate reacted with the hydroxide groups present on the surface of the BNC (highlighted by a blue dashed box in Figure 3). An attempt was made to quantify the relative amount of those chemical groups through the measurement of relative areas of each absorption band.[56] However, the scattering of the results prevented any significant conclusion. Finally, the presence of absorption bands of BNC nanoparticles was hindered due to the low concentration of BNC within the PUF and due to the overlapping of bands of BNC and PUF. These results are in agreement with the literature.[17–19,50,65,66]

Fracture Surface Analysis

The fractured surface of the PUF_{F1} at low magnifications (150×) is depicted in Figure 4 (left column). On the bottom left of the micrograph, the growth direction is specified. The statistical analysis of the cell dimensions, apparent density and other relevant measurements are reported in Table I, including the cell dimension on the parallel (L) and perpendicular (T) directions with respect to the growth direction as well as the anisotropy factor (AF), which was defined as the ratio of the dimension parallel to the growth direction to the perpendicular one. At low magnifications (150×), the size and geometry of the cell windows and how each cell intersected each other forming the cell struts was distinguished. The PUF_{F1} had an anisotropic morphology, a feature to be expected due to the molded nature of the PUF. The cell size had an average value of 383 µm in the longitudinal direction (L). The measured AF was 1.47, then, the cells were orientated parallel to the direction of foam growth. A magnified figure showing a typical cell strut of the PUF_{F1} is depicted in Figure 5(a,b). Within the strut, it is possible to distinguish that, during fracture, the cracks propagated with a very fragile nature, leaving behind no parabolic footprints or other relevant crack propagation features. In addition, at higher magnifications [Figure 5(b)], it can be discerned that the interpenetrating network was orientated towards the lateral ends of the struts. The previously described morphology represented what its typically found in semi-rigid or rigid PUFs.[1,67] On the other hand, the fractured surface of the PUF_{F1}-BNC 0.2 wt % is depicted in Figure 4 (right column) and Figure 5(c–h). As far as the cell dimensions statistics are concerned, it was found that the PUFs prepared with BNC had higher cell dimensions. In the L direction, the cells were +37.9% bigger (528 µm). The cell dimensions had a more heterogeneous nature due to the fact that its standard deviation was higher. In addition, the AF increased significantly, by +46.9%. Both of these measurements indicated that the BNC did not behave as a nucleation agent. On the contrary, it can be deduced that the incorporation of BNC in the formulation facilitated the formation of bigger cells regardless of the growth direction but with a more heterogeneous distribution. Another relevant feature was found within the struts when they were observed at higher magnifications [Figure 5(e,f)]. A conglomeration of cells with nanometric dimensions (nanocells) was found surrounding the clusters of BNC nanoparticles. These nanocells were absent in the PUF_{F1}. Such type of cells were found by Bandarian *et al.*[58] and it was assumed that its formation was due to the reaction of isocyanate with either carboxylic or hydroxide groups present on the surface of the nanoparticle which generated gaseous residues incapable of forming bigger cells. Previous work by our institute focusing on the characterization of BNC nanoparticles[34] revealed the presence of carboxylic functionalities, hence, we assume that this was the reason why such nanocells were formed.

It is important to compare these results with the measured apparent density. Taking into account those results, it can be inferred that both measurements are in agreement (apparent density and cell size). At first sight, this deduction seems not logical because it is generally accepted that nanoparticles act as nucleating agents, with a consequent increase of PUF density.[64] In PUFs formulated with CNC (no BNC publications are available), both an increase, a null and a decrease of PUF density have been reported.[49,50,52,53,56] Bandarian *et al.*,[58] Harikrishnan *et al.*,[69] and Kim *et al.*[70] found that the incorporation of multiwall carbon nanotubes, carbon nanofibers, and nanoclay decreased the density of the PUF. Taking into account these

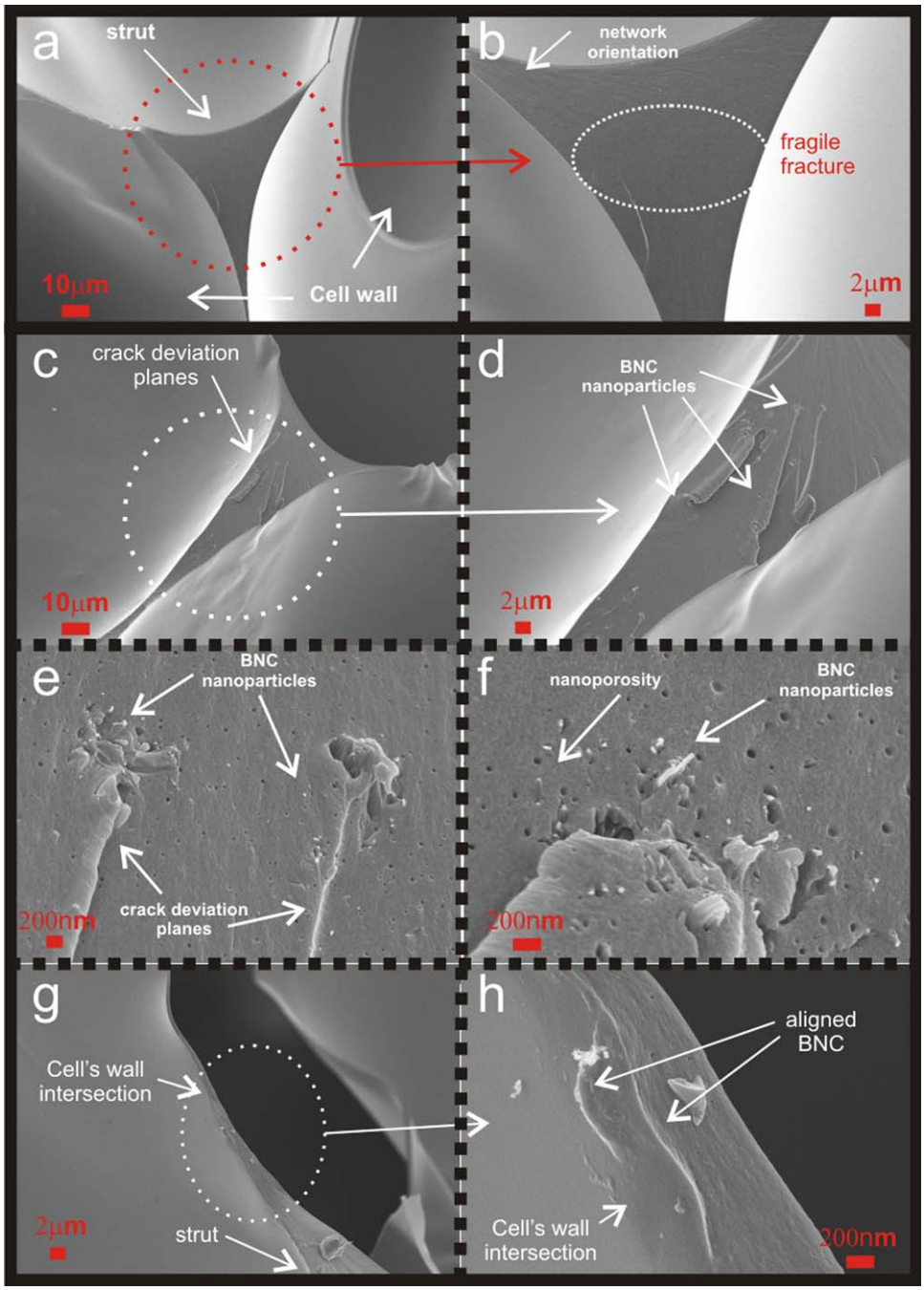

Figure 5. SEM images of the fracture surface of PUF_{F1}. (a) Cell strut, (b) magnified cell strut and PUF_{F1}-BNC 0.2 wt %, (c,d) strut and magnified strut, (e,f) magnified versions of conglomerated BNC nanoparticles and nanocells. (g,h) Cell wall intersection showing the alignment of BNC nanoparticles. [Color figure can be viewed at wileyonlinelibrary.com]

results, the decrease in density and the increase of cell size of the PUFs can be ascribed to a reduced potential nucleant density and to the ability of the BNC nanoparticles to avoid film drainage and rupture during cell growth, leading to the formation of the nanocells. One possible argument against this hypothesis is that the incorporation of BNC in the formulation could also introduce water (blowing agent) in the system. However, this argument is not supported by the fact that the T_{peak} of the PUFs reinforced with BNC was always lower (Table I). It is known that the reaction of water with isocyanate is highly exothermic.[1]

As far as the fracture surface is concerned, from Figure 5(c–h) it can be inferred that the incorporation of BNC in the formulation caused a substantial change of the fracture modes. First, it is important to highlight how the BNC was spatially distributed within the PUF. In the struts [Figure 5(c,d)], the BNC nanoparticles conglomerated in a well-distributed fashion,

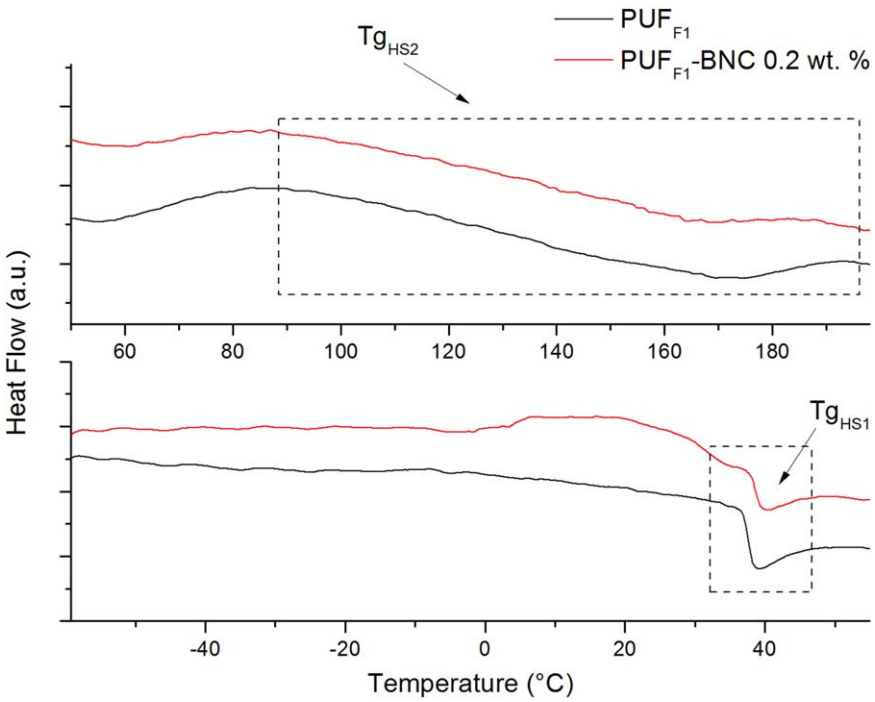

Figure 6. Heat flow as a function of temperature for the PUF_{F1} and the PUF_{F1}-BNC 0.2 wt %. [Color figure can be viewed at wileyonlinelibrary.com]

showing a good nanometric dispersion of the nanoparticles. A higher magnification [Figure 5(e,f)] showed clearly that the BNC tended to form well-dispersed clusters which were the cause of the formation of additional crack deviation planes. This higher density of fracture planes indicated that the fragile nature of the PUF_{F1} was significantly reduced. Another relevant observation can be deduced from Figure 5(g,h). The intersection of the cell walls was also populated by BNC nanoparticles. Within these regions, the BNC nanoparticles were oriented parallel to the thickness of the intersection of the cell walls. Assuming that the thickness of the PUF cell wall is much smaller with respect to the dimensions of a typical strut, it can be inferred that the effect of the BNC located in the cell walls on the mechanical properties of the PUF should be enhanced. This is strictly associated to the fact that the effective weight concentration of the BNC within the cell wall should be much higher with respect to the concentration of the BNC which is found in the strut. On the other hand, it is relevant to emphasize on the orientation of the BNC nanoparticles. The orientation was parallel to the cell wall. This specific orientation is of utmost importance so as to have a substantial effect on the mechanical properties of the nanocomposite foam. Using any model available in literature,[71] it is logical to deduce that an orientation parallel to the cell wall could be interpreted as a nanocomposite where the reinforcement (BNC) is orientated in the 0° direction and with a high volumetric reinforcement fraction. On the other hand, within the strut, the BNC can be orientated but this orientation is not as relevant because the volumetric reinforcement fraction is closer to the bulk value (0.2 wt %). Then, from these experimental observations, it can be deduced that the PUF_{F1} formulated with BNC should have an improved mechanical behavior with respect to the PUF_{F1}.

Differential Scanning Calorimetry

The heat flow as a function of temperature of the PUFs prepared in this work are depicted in Figure 6. The top figure showed the measurement within the temperature range 50 °C up to 200 °C while the bottom figure showed the temperature range −60 °C up to 50 °C. Two glass transitions were measured within the studied range. One transition was centered at approximately 40 °C and it covered a very narrow temperature region of less than 20 °C. The other one covered a wide temperature range, starting at approximately 90 °C and going up to 170 °C. No other thermal transitions were found. In addition, the thermal transitions were also measured for both the PUF_{F1} and the PUF_{F1}-BNC 0.2 wt %. No significant changes of the position of those thermal transitions were measured as a function of the incorporation of BNC in the formulation. Both thermal transitions can be associated to the HS of the microstructure of the PUF. Taking into account that two transitions were found, it can be deduced that the HS of the PUF had two different molecular structures. The transition centered at approximately 40 °C, denominated Tg_{HS1}, should be ascribed to a HS composed mainly of physically crosslinked urethane molecules. On the other hand, the high temperature transition, denominated Tg_{HS2}, can be associated to a HS composed of physically crosslinked urea and isocyanurate networks. Further analysis of the effects of these transitions on the thermomechanical properties of the PUF will be discussed below.

Mechanical Tests

The specific compressive elastic modulus ($E_c.\rho_{avg}^{-1}$) and strength ($\sigma_c.\rho_{avg}^{-1}$) are reported in Table I. If the reader is interested in the absolute values, the ρ_{avg} are also reported there. From the results it can be deduced that the incorporation

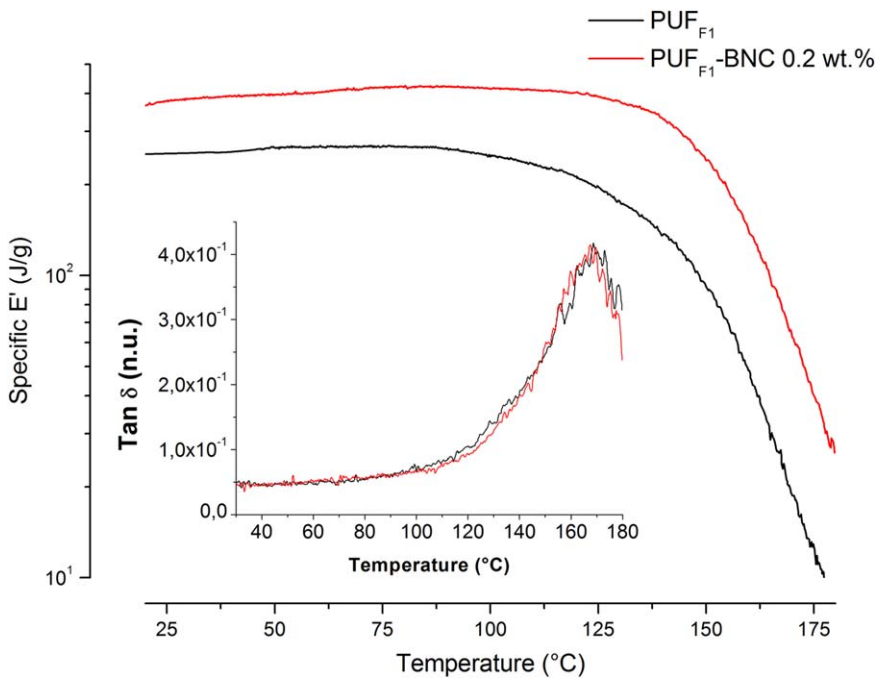

Figure 7. Specific storage modulus and damping factor (inset) for the PUF_{F1} and the PUF_{F1}-BNC 0.2 wt % under compression. [Color figure can be viewed at wileyonlinelibrary.com]

of BNC in the formulation caused an improvement of the specific modulus and strength by +4.67% and +23.6%, respectively. These results support the hypothesis that the BNC behaved as a HS, improving the mechanical properties of the resulting foam. Further support of this hypothesis was also found by thermogravimetric analysis, where a high WL centered at 300 °C indicated a higher specific content of HS in the PUF formulated with BNC. It is not possible to compare the results found in this work with others because this is the first publication using BNC in PUFs.

For the case of a PUF reinforced with 0.75 wt % of CNC, Li *et al.*[52] found substantial improvements of the mechanical properties of very high density PUFs (536 kg m^{-3}). The specific compressive modulus and strength were 17.01 J/g and 0.66 J/g, respectively. Comparing those results, it can be inferred that BNC is more effective in increasing the specific strength rather than the specific modulus. Even at a very low concentration (0.2 wt %), the specific strength was substantially higher. This tendency was also corroborated by recent results of Zhou *et al.*,[47] where a PUF was reinforced with CNC at 0.4 wt %.

Dynamical Mechanical Thermal Analysis

The specific storage modulus ($E'.\rho^{-1}$) and the damping factor (tan δ) as a function of temperature for the PUF_{F1} and the PUF_{F1}-BNC 0.2 wt % under compression are shown in Figure 7. The graph shows the average values of four different samples. Before analyzing the experimental results, it is important to emphasize that the measurements were performed under compression. During heating, the sample will expand in the direction of growth, which coincides with the direction where the compressive load was applied. Density will decrease, causing an increase of the specific E' as a function of temperature. If the thermomechanical properties of the polymer did not change, a positive slope of the E' versus temperature would be measured. Indeed, in Figure 7, the specific E' of the PUF_{F1} presented a stable value with a slightly positive slope up to temperatures of approximately 84 °C. From that temperature (84 °C) upwards, a steep decrease of the specific E' was observed. This relevant change of the specific E' can be associated to the glass transition temperature of the HS. Comparing this result with DSC analysis, there seems to be a contradiction because the Tg_{HS1} (centered at approximately 40 °C) measured with DSC is absent in the DMA analysis. This apparent contradiction has to do with how the DMA measurements were performed. For the case of the compressive analysis, the decrease of thermomechanical

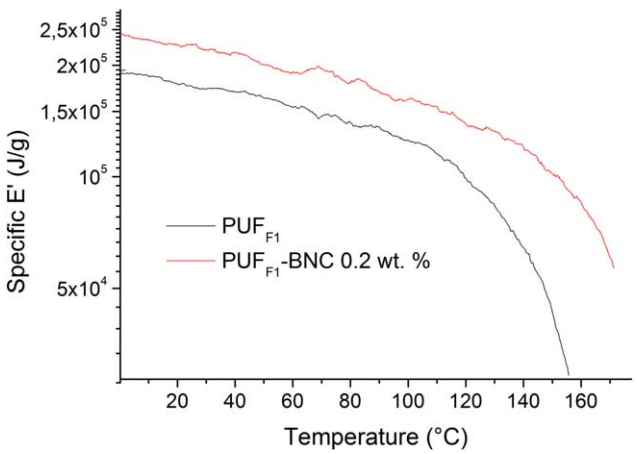

Figure 8. Specific storage modulus (E') as a function of temperature for the PUF_{F1} under flexural conditions. [Color figure can be viewed at wileyonlinelibrary.com]

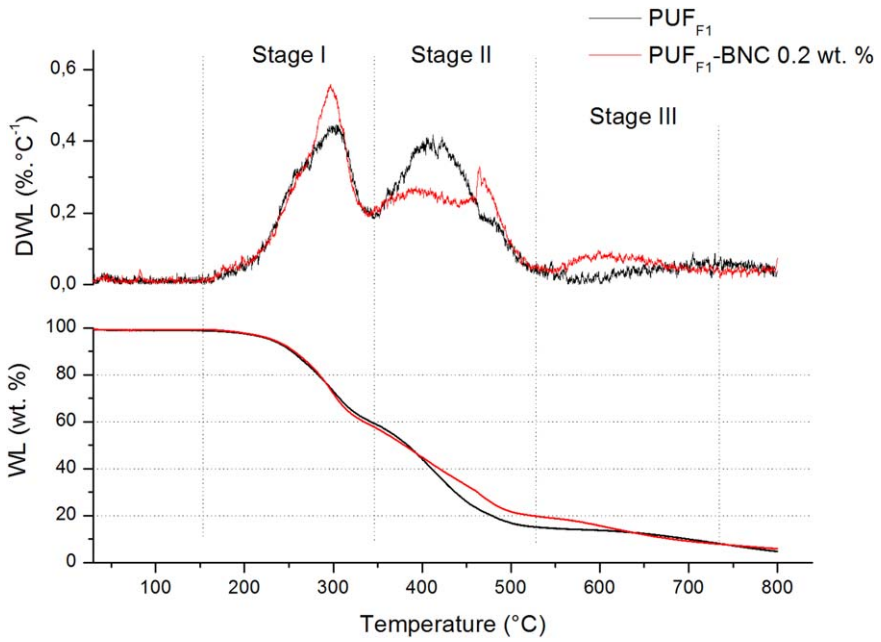

Figure 9. WL and DWL of PUFs as a function of temperature for the PUF_{F1} and the PUF_{F1}-BNC 0.2 wt %. [Color figure can be viewed at wileyonlinelibrary.com]

properties caused by the transition Tg_{HS1} was of a much less extent in comparison to geometrical effects. To corroborate this hypothesis, additional measurements were performed in the flexural mode (Figure 8), where the expansion of the PUF was perpendicular to the applied dynamic load. From those results, the effect of the Tg_{HS1} on the specific E' was effectively discerned, giving additional support to the hypothesis established above.

As far as the damping factor is concerned (Figure 7 inset), only one maximum was measured at elevated temperatures. Assuming that the maximum corresponded to the Tg_{HS}, its value can be assigned to 168 °C. On the other hand, the effect of the incorporation of BNC in the formulation can also be evaluated from Figure 7. A significant upward shift of the specific E' while maintaining a similar damping factor plot was measured. As a matter of fact, at 30 °C, the E' of the PUF_{F1}-BNC 0.2 wt % was +52.4% higher (387 J/g) than the E' of PUF_{F1}. In addition, the specific E' maintained a stable value up to temperatures of approximately 120 °C, indicating that the PUF_{F1} formulated with BNC maintained its mechanical properties up to much higher temperatures (+36 °C). Finally, the specific E' decreased less steeply as a function of temperature for the PUF formulated with BNC. All these results support the fact that the PUF formulated with BNC had an enhanced thermomechanical behavior. However, the fact that the damping factor showed no significant changes as a function of BNC content indicated that the formation of additional urethane groups due to the chemical reaction of the isocyanate and the BNC did not have a substantial effect on the damping properties of the material.

It is difficult to compare the results obtained in this work with what is available in literature. The main reason is that no other publication has dealt with the incorporation of BNC in PUFs. In addition, most publications compare mechanical results obtained in compression mode with thermomechanical properties in other modes (torsional or tensile). Nonetheless, Li *et al.*[52] studied the incorporation of CNC in PUFs at 0.75 wt %. The damping factor showed a similar trend to what we have found in our work, where the incorporation of CNC did not modify the position and height of the damping factor. In addition, an increase of the E' was found; however, those values were not normalized with respect to the foam density, preventing further analysis. Other articles have also studied the thermomechanical properties of PUFs with CNC.[32,55]

Thermogravimetric Weight Loss of the PUFs

The weight loss (WL) and the absolute value of the differential weight loss (DWL) of the PUFs prepared in this work as a function of temperature are depicted in Figure 9. The results showed the typical behavior associated to PUFs obtained from MDI isocyanate and castor oil polyol.[3,4,72] Three relevant thermal degradation stages were found and depicted in Figure 9. Stage I covered the temperature region 200 °C to 350 °C and it was associated to the decomposition of the urethane bond (HS) into isocyanate and alcohol, as well as amines and CO_2. The incorporation of BNC in the formulation had a relevant effect within this stage. Specifically, the DWL increased significantly for the case of the PUF_{F1}-BNC 0.2 wt %. This result reinforced the hypothesis that the PUF prepared with BNC had a higher content of urethane groups per unit volume. In addition, it can also be deduced that the incorporation of BNC in the formulation caused an increase of the relative amount of HS within the microstructure. On the other hand, from a thermal stability point of view, this represented a drawback because a higher specific content of urethane groups is associated to a microstructure with a lower thermal stability.

The weight loss during stage II covered the temperature range 350 to 550 °C and it was associated mainly to the

decomposition of the SS.[3] Stage II has associated a main decomposition rate process at 420 °C as mentioned but also a secondary decomposition rate process at about 480 °C related to a third stage of urethane degradation. Within this range, the incorporation of BNC in the formulation caused a significant reduction of the DWL and a change in the relative rate of the decomposition of the two above-mentioned processes. This result was to be expected because if a constant amount of isocyanate groups was present, an increase of the specific HS content should follow a decrease of the specific content of SS. Finally, stage III represented the WL associated to the decomposition of C—C bonds and decomposition products of stages I and II. In the PUF_{F1}-BNC 0.2 wt % sample the decomposition of some of the intermediate products occurred at higher temperature, indicating more stable structures formed in this case. Even though an increase of the DWL was measured, it was difficult to obtain any further deduction because the decomposition of stages I and II interfere with this stage.[3]

CONCLUSIONS

Semirigid polyurethane foams reinforced with BNC were successfully prepared at a fixed concentration of 0.2 wt %. Even at this very low concentration, the BNC had substantial effects on the foaming behavior, the physical, and the thermomechanical properties of the resulting foam. The incorporation of BNC caused a monotonous decrease of the cream time and a simultaneous decrease of the T_{peak}, indicating that the hydroxyls present on the surface of the BNC reacted with the isocyanate groups, forming additional urethane groups. FTIR and TGA analysis also supported this hypothesis. The incorporation of BNC caused a slight decrease of the apparent density (no nucleation effect) and a substantial increase of the cell size dimensions, producing a more heterogeneous distribution of cells and a substructure of nanocells within the struts of the PUF. Regardless of structural chemical changes, it is believed that this was the main cause for the improvement of the specific mechanical properties, such as compressive strength, modulus as well as thermomechanical ones. Other secondary causes were related to the formation of a higher urethane weight content, the alignment of the BNC nanoparticles within the cell walls and the formation of additional crack deviation planes. Comparing the results with literature, it was possible to conclude that BNC was particularly effective in increasing more the specific strength instead of the specific modulus. TGA analysis revealed that the addition of BNC in the PUF caused a decrease of the thermal stability of the resulting foam. This result was expected because an increase of the urethane weight content is certainly associated to a deteriorated thermal stability.

All the previous conclusions highlight and reinforce the hypothesis that the BNC nanoparticles can be used to formulate PUFs with an increased content of HS. Hence, the results of this work can be used to reformulate the PUF in order to have a higher content of precursors obtained from renewable resources.

Future work will focus on the effect of different processing routes to obtain PUFs reinforced with BNC. In addition, kinetic studies regarding the activity of surface functionalities of the BNC with isocyanates will also serve to have a further insight in this research area.

ACKNOWLEDGMENTS

The authors thank colleagues which indirectly contributed to this work, Analía Vazquez, Matías Nonna (Huntsman), Inés Bergamini (Resikem), Rafael Goldman (Mentvil), and A. Cordero (INIFTA).

REFERENCES

1. Randall, D.; Lee, S. The Polyurethanes Book; Wiley: New Jersey, **2003**.
2. Miao, S.; Wang, P.; Su, Z.; Zhang, S. *Acta Biomater.* **2014**, *10*, 1692.
3. Corcuera, M.; Rueda, L.; d'Arlas, B. F.; Arbelaiz, A.; Marieta, C.; Mondragon, I.; Eceiza, A. *Polym. Degrad. Stabil.* **2010**, *95*, 2175.
4. Javni, I.; Petrović, Z. S.; Guo, A.; Fuller, R. *J. Appl. Polym. Sci.* **2000**, *77*, 1723.
5. Juntaro, J.; Ummartyotin, S.; Sain, M.; Manuspiya, H. *Carbohydr. Polym.* **2012**, *87*, 2464.
6. Lligadas, G.; Ronda, J. C.; Galià, M.; Caḍiz, V. *Biomacromolecules* **2010**, *11*, 2825.
7. Delebecq, E.; Pascault, J. P.; Boutevin, B.; Ganachaud, F. *Chem. Rev.* **2012**, *113*, 80.
8. Fenouillot, F.; Rousseau, A.; Colomines, G.; Saint-Loup, R.; Pascault, J. P. *Prog. Polym. Sci.* **2010**, *35*, 578.
9. Hojabri, L.; Kong, X.; Narine, S. S. *Biomacromolecules* **2009**, *10*, 884.
10. Rueda, L.; Fernández d'Arlas, B.; Zhou, Q.; Berglund, L. A.; Corcuera, M. A.; Mondragon, I.; Eceiza, A. *Compos. Sci. Technol.* **2011**, *71*, 1953.
11. Gao, X.; Zhou, B.; Guo, Y.; Zhu, Y.; Chen, X.; Zheng, Y.; Gao, W.; Ma, X.; Wang, Z. *Colloids Surf. A* **2010**, *371*, 1.
12. Herrera-Alonso, J. M.; Marand, E.; Little, J. C.; Cox, S. S. *J. Membr. Sci.* **2009**, *337*, 208.
13. Salahuddin, N.; Abo-El-Enein, S. A.; Selim, A.; Salah El-Dien, O. *Appl. Clay Sci.* **2010**, *47*, 242.
14. Százdi, L.; Pozsgay, A.; Pukánszky, B. *Eur. Polym. J.* **2007**, *43*, 345.
15. Aranguren, M. I.; Marcovich, N. E.; Salgueiro, W.; Somoza, A. *Polym. Test.* **2013**, *32*, 115.
16. Ke, Y. C.; Stroeve, P. Polymer-Layered Silicate and Silica Nanocomposites; Elsevier: Amsterdam, The Netherlands, **2005**.
17. Kaushik, A.; Ahuja, D.; Salwani, V. *Compos. A* **2011**, *42*, 1534.
18. Özgür Seydibeyoğlu, M.; Oksman, K. *Compos. Sci. Technol.* **2008**, *68*, 908.
19. Rueda, L.; Saralegui, A.; Fernández d'Arlas, B.; Zhou, Q.; Berglund, L. A.; Corcuera, M. A.; Mondragon, I.; Eceiza, A. *Carbohydr. Polym.* **2013**, *92*, 751.
20. Chen, G. D.; Zhou, S. X.; Liao, H. M.; Wu, L. M. *J. Compos. Mater.* **2005**, *39*, 215.

21. Ke, Y. C.; Stroeve, P. Polymer-Layered Silicate and Silica Nanocomposites, 1st ed.; Elsevier Science: Amsterdam, The Netherlands, **2005**.
22. Chidichimo, G.; Aloise, A.; Beneduci, A.; De Rango, A.; Pingitore, G.; Furgiuele, F.; Valentino, P. *Polym. Compos.* **2015**, *37*, 3042.
23. Wang, Y.; Zhang, C.; Ren, L.; Ichchou, M.; Galland, M. A.; Bareille, O. *Polym. Compos.* **2013**, *34*, 1847.
24. Palanisamy, A. *Polym. Compos.* **2013**, *34*, 1306.
25. Brinchi, L.; Cotana, F.; Fortunati, E.; Kenny, J. *Carbohydr. Polym.* **2013**, *94*, 154.
26. Charreau, H.; L Foresti, M.; Vázquez, A. *Recent Pat. Nanotechnol.* **2013**, *7*, 56.
27. Dong, X. M.; Revol, J. F.; Gray, D. G. *Cellulose* **1998**, *5*, 19.
28. Eichhorn, S. J.; Dufresne, A.; Aranguren, M.; Marcovich, N.; Capadona, J.; Rowan, S. J.; Weder, C.; Thielemans, W.; Roman, M.; Renneckar, S. *J. Mater. Sci.* **2010**, *45*, 1.
29. Iguchi, M.; Yamanaka, S.; Budhiono, A. *J. Mater. Sci.* **2000**, *35*, 261.
30. Khalil, H. A.; Davoudpour, Y.; Islam, M. N.; Mustapha, A.; Sudesh, K.; Dungani, R.; Jawaid, M. *Carbohydr. Polym.* **2014**, *99*, 649.
31. Revol, J. F.; Bradford, H.; Giasson, J.; Marchessault, R.; Gray, D. *Int. J. Biol. Macromol.* **1992**, *14*, 170.
32. Saralegi, A.; Rueda, L.; Martin, L.; Arbelaiz, A.; Eceiza, A.; Corcuera, M. *Compos. Sci. Technol.* **2013**, *88*, 39.
33. Thakur, V. K.; Thakur, M. K. *Carbohydr. Polym.* **2014**, *109*, 102.
34. Vazquez, A.; Foresti, M. L.; Cerrutti, P.; Galvagno, M. *J. Polym. Environ.* **2013**, *21*, 545.
35. Guise, C.; Fangueiro, R. ICNF2015–2st International Conference on Natural Fibers; Azores, Portugal, **2015**.
36. HPS, A. K.; Saurabh, C. K.; Adnan, A.; Fazita, M. N.; Syakir, M.; Davoudpour, Y.; Rafatullah, M.; Abdullah, C.; Haafiz, M.; Dungani, R. *Carbohydr. Polym.* **2016**, *150*, 216.
37. Li, F.; Mascheroni, E.; Piergiovanni, L. *Pack. Technol. Sci.* **2015**, *28*, 475.
38. Serpa, A.; Velásquez-Cock, J.; Gañán, P.; Castro, C.; Vélez, L.; Zuluaga, R. *Food Hydrocolloids* **2016**, *57*, 178.
39. Hoeng, F.; Denneulin, A.; Bras, J. *Nanoscale* **2016**, *8*, 13131.
40. Astley, O. M.; Chanliaud, E.; Donald, A. M.; Gidley, M. J. *Int. J. Biol. Macromol.* **2003**, *32*, 28.
41. Vandamme, E.; De Baets, S.; Vanbaelen, A.; Joris, K.; De Wulf, P. *Polym. Degrad. Stabil.* **1998**, *59*, 93.
42. Ramírez, J. A.; Suriano, C. J.; Cerrutti, P.; Foresti, M. L. *Carbohydr. Polym.* **2014**, *114*, 416.
43. Vazquez, A.; Foresti, M. L.; Moran, J. I.; Cyras, V. P. Handbook of Polymer Nanocomposites. Processing, Performance and Application; Springer: Berlin, Heidelberg, **2015**.
44. Cerrutti, P.; Roldán, P.; García, R. M.; Galvagno, M. A.; Vázquez, A.; Foresti, M. L. *J. Appl. Polym. Sci.* **2016**, *133*, DOI: 10.1002/app.43109.
45. Menchaca-Nal, S.; Londoño-Calderón, C. L.; Cerrutti, P.; Foresti, M. L.; Pampillo, L.; Bilovol, V.; Candal, R.; Martínez-García, R. *Carbohydr. Polym.* **2016**, *137*, 726.
46. Oksman, K.; Aitomäki, Y.; Mathew, A. P.; Siqueira, G.; Zhou, Q.; Butylina, S.; Tanpichai, S.; Zhou, X.; Hooshmand, S. *Compos. A* **2016**, *83*, 2.
47. Zhou, X.; Sain, M. M.; Oksman, K. *Compos. A* **2016**, *83*, 56.
48. Luo, F.; Wu, K.; Guo, H.; Zhao, Q.; Liang, L.; Lu, M. *J. Therm. Anal. Calorimetry* **2015**, *122*, 717.
49. Hussain, M.; Nakahira, A.; Niihara, K. *Mater. Lett.* **1996**, *26*, 185.
50. Lobos, J.; Velankar, S. *J. Cell. Plast.* **2016**, *52*, 57.
51. Li, Y.; Ragauskas, A. J. *Algae* **2011**, *75*, 10.
52. Li, Y.; Ren, H.; Ragauskas, A. J. *Nano-Micro Lett.* **2010**, *2*, 89.
53. Li, Y.; Ren, H.; Ragauskas, A. J. *J. Nanosci. Nanotechnol.* **2011**, *11*, 6904.
54. Faruk, O.; Sain, M.; Farnood, R.; Pan, Y.; Xiao, H. *J. Polym. Environ.* **2014**, *22*, 279.
55. Mosiewicki, M. A.; Rojek, P.; Michałowski, S.; Aranguren, M. I.; Prociak, A. *J. Appl. Polym. Sci.* **2015**, *132*, DOI: 10.1002/app.41602.
56. Cordero, A. I.; JavierFortunati, E.; Kenny, J. M.; Chiacchiarelli, L. M. *Carbohydr. Polym.* **2015**, *134*, 110.
57. Lee, Y. J.; Park, C. K.; Kim, S. H. *Polym. Compos.* **2016**.
58. Seydibeyoğlu, M.; Misra, M.; Mohanty, A.; Blaker, J. J.; Lee, K. Y.; Bismarck, A.; Kazemizadeh, M. *J. Mater. Sci.* **2013**, *48*, 2167.
59. Pinto, E. R. P.; Barud, H. S.; Polito, W. L.; Ribeiro, S. J. L.; Messaddeq, Y. *J. Therm. Anal. Calorimetry* **2013**, *114*, 549.
60. Johnson, M.; Shivkumar, S. *J. Appl. Polym. Sci.* **2004**, *93*, 2469.
61. Kenny, J. M.; Torre, L.; Chiacchiarelli, L. M. *J. Appl. Polym. Sci.* **2015**, *132*, DOI: 10.1002/app.42750.
62. Hestrin, S.; Schramm, M. *Biochem. J.* **1954**, *58*, 345.
63. Chiacchiarelli, L. M.; Puri, I.; Puglia, D.; Kenny, J. M.; Torre, L. *Colloid Polym. Sci.* **2013**, *291*, 2745.
64. Rothon, R. Particulate-Filled Polymer Composites; iSmithers Rapra Publishing, **2003**.
65. Rials, T. G.; Wolcott, M. P.; Nassar, J. M. *J. Appl. Polym. Sci.* **2001**, *80*, 546.
66. Silva, R. V.; Spinelli, D.; Bose Filho, W. W.; Claro Neto, S.; Chierice, G. O.; Tarpani, J. R. *Compos. Sci. Technol.* **2006**, *66*, 1328.
67. Szycher, S. Szycher's Handbook of Polyurethanes; CRC Press LLC: New York, USA, **1999**.
68. Bandarian, M.; Shojaei, A.; Rashidi, A. M. *Polym. Int.* **2011**, *60*, 475.
69. Harikrishnan, G.; Singh, S. N.; Kiesel, E.; Macosko, C. W. *Polymer* **2010**, *51*, 3349.
70. Kim, S.; Lee, M.; Kim, H.; Park, H.; Jeong, H.; Yoon, K.; Kim, B. *J. Appl. Polym. Sci.* **2010**, *117*, 1992.
71. Barbero, E. J. Introduction to Composite Materials Design; CRC Press: New York, **2010**.
72. Husić, S.; Javni, I.; Petrović, Z. S. *Compos. Sci. Technol.* **2005**, *65*, 19.